Pulsed Electron Beam For Electric Potential Sensing And Control

Julian Hammerl and Hanspeter Schaub

***Abstract*—Remotely estimating the electric potential of nearby spacecraft is valuable for spaceflight as it may prevent electrostatic discharges during docking and can reduce the control effort during proximity operations with charged spacecraft. Two promising methods that utilize an electron that is emitted from a servicing satellite and aimed at the target spacecraft have been developed to remotely estimate the potential of the target. However, the two methods benefit from dissimilar electron beam parameters. To create conditions that improve the signal for both methods, it is proposed to pulse the electron beam to quickly switch between two sets of favorable beam parameters. This work investigates control algorithms that adjust the duty cycle (ratio of time between two beam settings) for different types of beam pulsing to measure and control the potential of the target spacecraft. The results suggest that pulsing the beam can be beneficial for the sensing methods.**

I. Introduction

Most research on spacecraft charging focuses on the effects of only the space environment, that is, how much a spacecraft charges naturally due to the ambient plasma environment. Spacecraft charging induced by electron beam impact, electron beam emission, and ion beam emission has received little attention [1]–[4]. Recently, the coupled effect of a continuous electron beam on the electric potentials of two neighboring spacecraft was studied in more detail [5]. Besides studying the varying transient charging behaviors due to multiple equilibria, the work also investigated the impact of the electron beam current on remote sensing methods that estimate the electric potential of another spacecraft. Remotely sensing the electric potential of a nearby spacecraft is valuable for spaceflight as it provides a warning for probable electric discharges during docking and reduces the control effort during rendezvous and proximity operations with charged spacecraft [6], [7]. Two promising remote electric potential sensing methods have been proposed [8], [9]. Both methods utilize an electron gun that is attached to a servicing satellite. The electron gun is aimed at a target object and excites secondary electrons and x-rays from the target which are used to estimate the potential.

The sensing methods benefit from electron beam configurations that conflict each other. A lower electron beam energy is beneficial for the electron method, as more secondary electrons are excited if the impact energy of the electron beam on the target spacecraft is only a few kilo-volts. A high electron beam current is preferred as it will yield more secondary electrons and consequently a stronger signal. The x-ray method benefits from a higher beam energy, as the resulting higher electron beam impact energy causes x-rays to be emitted with a wider energy spectrum, allowing for more materials to be identified and generally better performance because the impact energy does not align with the characteristic energy of some x-rays. While the x-ray method also benefits from a higher electron beam current, resulting in more generated x-rays, some commercial-off-the-shelf x-ray detectors may saturate if too many x-rays are detected at once.

Julian Hammerl, Graduate Research Assistant at the University of Colorado Boulder. E-mail: julian.hammerl@colorado.edu

Hanspeter Schaub, Schaden Leadership Chair, Professor and Department Chair at the University of Colorado Boulder.

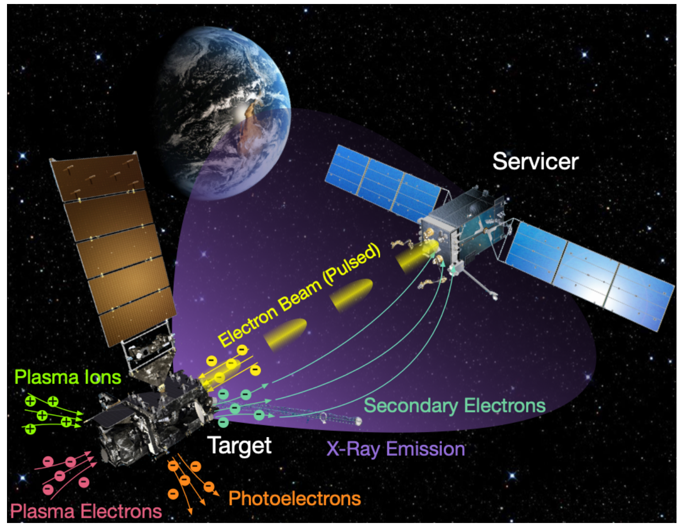

Fig. 1: Illustration of Spacecraft Charging and Electric Potential Sensing

Given the conflicting desired electron beam configurations, a pulsed beam is proposed to quickly switch between beam settings. For example, by alternating between a low and high electron beam energy, one can create conditions that, on average, are beneficial for both sensing methods. Good measurements from the electric potential sensing methods are an important factor for closed-loop charge control of a nearby spacecraft using an electron beam, but the changing beam parameters of a pulsed beam affect the charging response of the target spacecraft and consequently the control itself. However, a pulsed beam also provides more ways of charge control. For example, using the feedback from the potential measurements, the duty cycle (ratio of time between two beam settings) for the electron beam current or energy can be controlled to achieve a desired potential on the target.

II. Background

A. Remote Electric Potential Estimation

Two promising methods for the remote estimation of spacecraft electric potentials have been proposed, both of which utilize an electron beam that is emitted from a servicing spacecraft and aimed at a target spacecraft [8]–[13]. The electron beam is emitted with some initial kinetic energy, corresponding to the operating energy of the electron gun. As the beam travels from the servicer toward the target, it is slowed down (accelerated) if the target is charged negatively (positively). The impacting electrons on the target excite x-rays from the target surface that are emitted with a maximum energy up to the landing energy (impact energy) of the electron beam. Thus, the landing energy of the electron beam can be determined by finding the maximum emitted x-ray energy via x-ray spectroscopy. Because the change in kinetic energy of the electron beam corresponds to the electric potential difference between the two spacecraft, the electric potential of the target can be inferred if the potential of the servicer and initial beam energy are known and the landing energy of the electron beam is estimated using x-rays. This is referred to as the x-ray method [8], [10], [11]. The impacting electron beam also excites secondary electrons from the target surface, which are emitted with negligible initial kinetic energy. If the target is charged negatively and the servicer positively, these secondary electrons are accelerated towards the servicer, where the increase in kinetic energy of the secondary electrons corresponds to the electric potential difference between the two spacecraft. Thus, if the potential of the servicer is known and the energy of the secondary electrons as they arrive at the servicer is measured, the electric potential of the target can be inferred. This is referred to as the electron method [9], [12], [13].

The intensity of the x-ray and secondary electron signals strongly depend on the electron beam parameters, that is, the electron beam current I_{EB} and electron beam (operating) energy E_{EB}. The higher the beam current, the more electrons are impacting on the target and the more x-rays and secondary electrons are emitted from the target. Thus, a high beam current is preferred for a better signal, although the saturation of the x-ray detector (when too many x-rays are detected at once) should be considered. In terms of beam energy, a high beam energy that results in landing energies of at least 5-10 keV is preferred for the x-ray method. Characteristic x-ray peaks may interfere with the x-ray method if they are close to the landing energy (maximum energy in the x-ray spectrum). With a high landing energy, one can avoid that low-energy characteristic x-ray peaks (e.g. aluminum at 1.5 keV and titanium at 4.5 keV) are close to the maximum x-ray energy that is used for the estimation. Moreover, the wider energy spectrum of the x-rays allows for more materials to be identified. The electron method, on the other hand, benefits from a lower beam energy. The secondary electron yield (the average number of secondary electrons emitted per impacting primary electron) depends on the impact energy of the incoming electron. Although there are many uncertainties involved with the secondary electron yield, the maximum yield occurs at an impact energy of less than 1 keV for most materials [14, Chapter 3]. Above this specific energy, the secondary electron yield decreases continuously with increasing impact energy. Thus, a landing energy of only a few keV results in more secondary electrons being emitted from the target and consequently a stronger signal for the electron method. Another consideration for the beam parameters is the deflection of the electron beam due to the interaction with the electric field generated by the two charged spacecraft [15]. Unrelated to the signal produced, a high electron beam energy is beneficial because the electron beam is deflected less if it has a higher energy.

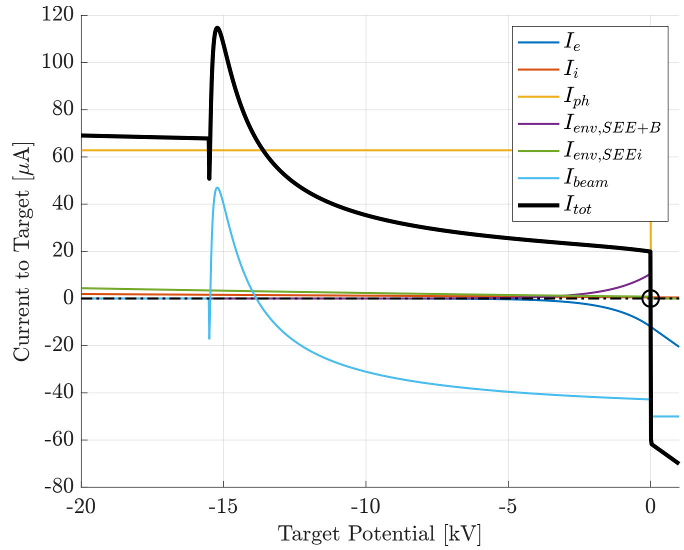

Fig. 2: Currents vs. Potential of Target. $I_{EB} = 50$ μA, $E_{EB} = 20$ keV, resulting servicer equilibrium potential of about $+4.5$ keV

B. Spacecraft Charging Model

The charging model is adopted from Ref. [5], which assumes spherical, fully conducting spacecraft. Thus, the spacecraft has only one electric potential ϕ (no differential charging). The following currents are considered for the target, with servicer potential ϕ_S and target potential ϕ_T:

- Plasma electron current, $I_e(\phi_T)$
- Plasma ion current, $I_i(\phi_T)$
- Photoelectric current, $I_{ph}(\phi_T)$
- Plasma electron induced secondary and backscattered electron current, $I_{\text{SEE},B,e}(\phi_T)$
- Plasma ion induced secondary electron current, $I_{\text{SEE},i}(\phi_T)$
- Electron beam current on target, $I_{EB,T}(\phi_T, \phi_S)$
- Electron beam induced secondary and backscattered electron current, $I_{\text{SEE},B,eb}(\phi_T, \phi_S)$

The total current on the target is

$$I_{\text{tot},T}(\phi_T, \phi_S) = I_e(\phi_T) + I_i(\phi_T) + I_{ph}(\phi_T) + I_{\text{SEE},B,e}(\phi_T) + I_{\text{SEE},i}(\phi_T) + I_{EB,T}(\phi_T, \phi_S) + I_{\text{SEE},B,eb}(\phi_T, \phi_S) \tag{1}$$

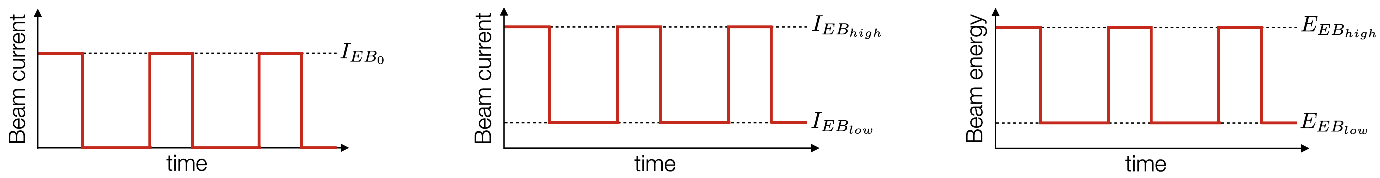

(a) On-Off Pulsing (b) Current Pulsing (c) Energy Pulsing

Fig. 3: Types of Pulsing

and the equilibrium potential of the target is found by determining the root of this equation. Using the naturally occurring currents

$$I_{\text{nat},T}(\phi_T) = I_e(\phi_T) + I_i(\phi_T) + I_{ph}(\phi_T) + I_{\text{SEE},B,e}(\phi_T) + I_{\text{SEE},i}(\phi_T) \quad (2)$$

and the electron beam induced currents

$$I_{\text{beam},T}(\phi_T, \phi_S) = I_{EB,T}(\phi_T, \phi_S) + I_{\text{SEE},B,eb}(\phi_T, \phi_S) \quad (3)$$

one can also rewrite Eq. (1) as

$$I_{\text{tot},T}(\phi_T, \phi_S) = I_{\text{nat},T}(\phi_T) + I_{\text{beam},T}(\phi_T, \phi_S) \quad (4)$$

In this work, the servicer potential is assumed to be controlled such that it remains at $\phi_S = 0$. The differential equation for the target potential is

$$\dot{\phi}_T = \frac{1}{C_T} I_{\text{tot},T}(\phi_T, \phi_S) \quad (5)$$

where C_T is the capacitance of the target spacecraft and affects how quickly the target charges.

The plasma is assumed to be single-Maxwellian, with the plasma environment data being taken from Ref. [16], which provides the electron and ion temperature and density (T_e, n_e, T_i, n_i) as a function of local time and K_p index. Local time represents the location in GEO, where a local time of 12 hours indicates that the spacecraft is between Sun and Earth, and a local time of 24 hours corresponds to the spacecraft being behind Earth. The K_p index, or planetary K-index, characterizes the intensity of geomagnetic storms. In this work, the plasma data for a K_p index of 2 and local time of 6 hours is used, resulting in $n_e = 0.95$ cm^{-3}, $T_e = 1400$ eV, $n_i = 0.75$ cm^{-3}, $T_i = 7100$ eV. The target is assumed to be eclipsed (no photoelectric current).

C. Electron Beam Pulsing

Three types of pulsing are considered: on-off pulsing, current magnitude pulsing, and beam energy pulsing. For on-off pulsing (Fig. 3a), the beam is periodically turned off, providing some nominal current $I_{EB,0}$ during the on-time and no current during the off-time. For current pulsing (Fig. 3b), the beam switches between a high beam current $I_{EB,\text{high}}$ and a low current $I_{EB,\text{low}}$. Finally, for energy pulsing (Fig. 3c), the beam alternates between a high beam energy $E_{EB,\text{high}}$ and a low energy $E_{EB,\text{low}}$. Current pulsing is equivalent to on-off pulsing if $I_{EB,\text{low}} = 0$. In a less obvious way, on-off pulsing can also be achieved under certain conditions with energy pulsing. If the low energy is smaller than the difference of electric potentials, i.e. $E_{EB,\text{low}} < \phi_S - \phi_T$, the beam is not energetic enough to reach the target [5]. This results in zero current due to the electron beam during the low energy period of the pulse cycle, and is consequently comparable to on-off pulsing. In addition to the low and high current/energy levels, two more parameters are needed to describe the pulsing cycle: the pulsing frequency f and the duty cycle d. The frequency is equal to

$$f = \frac{1}{T_{\text{pulse}}} \quad (6)$$

where $T_{\text{pulse}} = t_{\text{high}} + t_{\text{low}}$ is the period of one pulse cycle, t_{high} is the duration of the high cycle, and t_{low} is the duration of the low cycle. For on-off pulsing, t_{high} corresponds to the time that the beam is on and t_{low} to the time that the beam is off. The duty cycle is

$$d = \frac{t_{\text{on}}}{T_{\text{pulse}}} = \frac{t_{\text{on}}}{t_{\text{high}} + t_{\text{low}}} \quad (7)$$

and consequently $0 \leq d \leq 1$.

D. Electric Potential Control

While providing a way to actively sense the electric potential of the target by exciting x-rays and secondary electrons, the electron beam may also be used to control the potential of the servicer and target spacecraft. Using the estimated target potential, the electron beam current is adjusted to drive the target potential to a desired value. Alternatively, if the beam current is pulsed, the duty cycle can be controlled to change the resulting net beam current. While the electron beam energy determines how negatively the target can be charged and while it has some influence on the equilibrium potential of the target, it is not the most intuitive control variable.

III. Results

A. Open-Loop Pulsing

1) On-Off Pulsing: On-off pulsing is shown in Fig. 4 for different duty cycles and pulsing frequencies, and a nominal beam current of $I_{EB,0} = 10$ µ and beam energy $E_{EB} = 20$ keV. During the on-cycle, the beam charges the target as a continuous beam does. During the off-cycle, the beam current is zero, so the target recharges slightly towards its natural equilibrium potential. This essentially reduces the net current due to the electron beam. For on-off pulsing, the duty cycles reduces the effective beam current by approximately $I_{EB,\text{eff}} = d \cdot I_{EB,0}$ and consequently affects the obtained equilibrium potential. The frequency only determines the amplitude of the oscillations, but has no affect on what potential the target

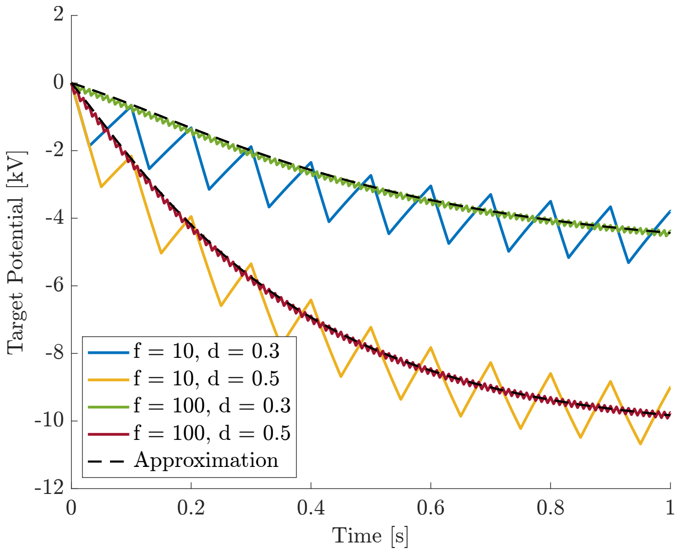

Fig. 4: Duty Cycle d and Pulsing Frequency f

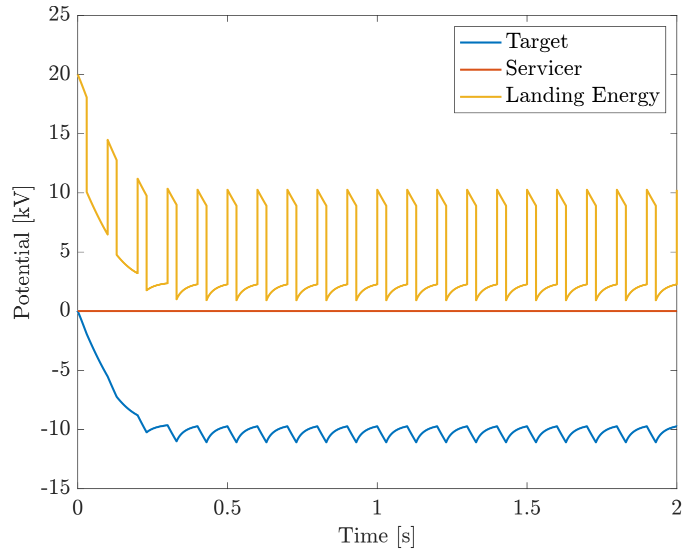

Fig. 5: Open Loop Energy Pulsing

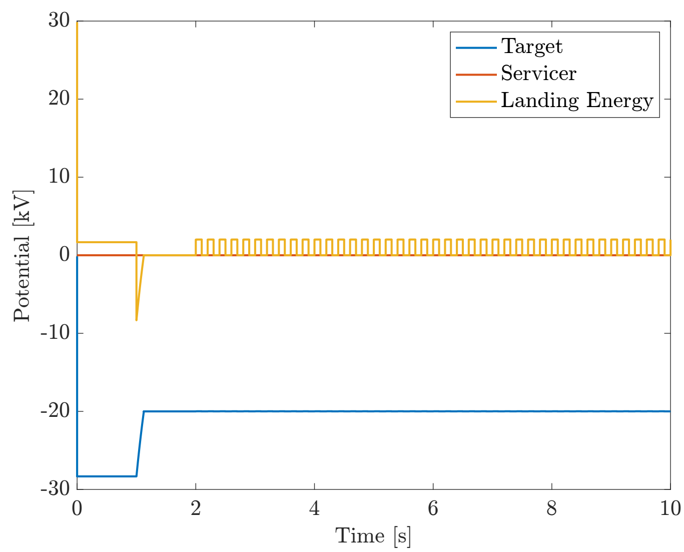

Fig. 6: Open Loop Potential Control

converges to. In Fig. 4, the Approximation lines correspond to a continuous beam with a current of $I_{EB} = I_{EB,\text{eff}}$.

For electric potential sensing purposes, on-off pulsing may be beneficial in multiple ways. First, when estimating the natural (no electron beam current) equilibrium potential of the target, any current from the electron beam affects the target potential itself. Thus, it is desired to keep the beam current as low as possible while still producing a sufficient x-ray and secondary electron signal to accurately measure the potential. By pulsing the electron beam, one can reduce the net beam current to levels below the capabilities of the electron gun for a continuous beam. Second, the excited x-rays and secondary electrons are emitted at a specific frequency (the pulsing frequency), allowing for band-pass filtering of the signal. Thus, for the same effective beam current, pulsing can provide a better signal-to-noise ratio. Finally, the pulsed beam can also increase the efficiency of the Electrostatic Tractor debris removal method [17], as it increases the average electrostatic force for the same power used for the electron beam [18].

2) Energy Pulsing: The drawback of on-off pulsing for electric potential sensing purposes is that it does not significantly affect the landing energy of the electron beam and therefor might only be well-suited for one estimation method. For example, in Fig. 4, the landing energy is between approximately 16 and 18 keV for $d = 0.3$ and between 10 and 12 keV for $d = 0.5$. Given that the servicer potential is held constant at 0 V and the beam energy is constant, the oscillations of the landing energy are purely a result of the oscillating target potential. Such high landing energies are only beneficial for the x-ray method, due to the limited number of secondary electrons being excited for this range of landing energies.

To alternate the landing energy between to levels that are favorable for one estimation method at a time, the beam energy can be pulsed, as shown in Fig. 5 for $d = 0.3$, $f = 10$ Hz and $I_{EB,0} = 10$ µA. The high beam energy is $E_{EB,\text{high}} = 20$ keV and the low beam energy is $E_{EB,\text{low}} = 12$ keV. At the beginning of the simulation, both beam energy levels result in landing energies above approximately 3 keV, which causes the target to charge negatively in either cycle. However, after about 0.3 seconds, the target potential stops decreasing and instead oscillates around -10 keV. During the high energy cycle, the target still charges negatively, and the corresponding landing energy of about 10 keV is beneficial for the x-ray method. However, during the low energy cycle, the landing energy is within a range where the secondary electron yield is greater than 1, causing the electron beam to actually charge the target positively. Due to the increased number of secondary electrons being excited, the low energy cycle is beneficial for the secondary electron method.

3) Open-Loop Potential Control: The aforementioned pulsing strategies may be beneficial for sensing purposes, but the change the potential of the target to an initially unknown value. It may be desired to charge the target to a specific potential.

The estimated potential could be used as feedback for a closed-loop control. However, recently, an open-loop control approach was suggested that takes advantage of the multiple equilibria that may exist for the target potential [5]. One of the stable equilibrium potentials is close to the point where the beam is just barely energetic enough to reach the target. If the potential is slightly less negative than the equilibrium, the beam is able to reach the target and charges it negatively until it reaches the equilibrium. If the potential is slightly more negative than the equilibrium, the beam is unable to reach the target (resulting in zero beam current), and the natural currents drive the potential back in the positive direction until the beam is hitting the target again. Thus, for a zero servicer potential, this equilibrium point of the target potential is approximately equal to the beam energy, but negative. The drawback of this control approach is that the landing energy is close approximately zero, so no x-rays or secondary electrons are excited, and no potential can be estimated. The resulting x-ray and secondary electron signal looks just like the beam is missing the target entirely. This ambiguity is quite significant: either the beam is hitting the target and the potential is equal to the beam energy (e.g. -20 kV), or the beam is missing the target and the potential is equal to the natural potential, which may even be around 0 V. Pulsing the beam between two energy levels can solve this ambiguity.

As shown in Fig. 6, the beam energy is 30 keV for one second, charging the target to about -28 kV, followed by a one second phase with an energy of 20 keV. Due to the decrease of beam energy, the beam is now unable to reach the target (negative landing energy in the figure). This brings the potential to the stable equilibrium around -20 kV where the 20 keV beam is just barely energetic enough to reach the target. Now, the beam is pulsed between energies of 20 and 22 keV, with $d = 0.5$, $f = 5$ Hz and $I_{EB,0} = 50$ µA. During the 20 keV phase, the potential is at -20 kV. During the 22 keV phase, the potential changes slightly, but the landing energy increases to about 2 keV. Thus, secondary electrons are excited that can be used for the estimation of the electric potential, and to ensure that the beam is hitting and charging the target spacecraft.

B. *Closed-Loop Pulsing*

The potential estimation from the sensing methods may also be used as feedback for a charge control to maintain a desired potential on the target. For on-off pulsing, the duty cycle can be controlled in a way such that the effective current delivered to the target results in the desired equilibrium potential. The simple feedback law

$$d_k = d_{k-1} + K_d(\hat{\phi}_T - \phi_{T,des}) \tag{8}$$

is used to update the duty cycle, where d_k and d_{k-1} are the duty cycles from the current and previous control period, respectively, K_d is the feedback gain, $\hat{\phi}_T$ is the most recent estimate of the target potential, and $\phi_{T,des}$ is the desired potential of the target. In this example, the control update rate is 1 Hz. Moreover, a method is implemented to simulate the estimation of the target potential. When only measuring one potential at a time (as opposed to multiple potentials, e.g. in the case of a differentially charged spacecraft), the x-ray method detects the potential corresponding to the highest landing energy in the recorded x-ray spectrum (the most positive or least negative electric potential) [11]. Thus, if the x-ray detector records x-rays over a certain time and the target potential changes during that time period (while the beam energy remains constant), the estimated potential corresponds to the least negative potential. Here, the estimation time window is 1 second, and the implemented estimation method simply take the highest potential during that time frame.

The simulation results for closed-loop on-off pulsing are shown in Fig. 7 for a desired potential of -3 kV and a feedback gain of $K_d = \cdot 10^{-5}$. The beam energy is 20 keV and the nominal beam current $I_{EB,0} = 10$ µA. Starting at 0 V and a duty cycle of less than 0.1, the duty cycle ramps up to achieve the desired potential of -3 kV. Because the simplified estimation method that is implemented in the simulation takes the highest potential as the measurement, the converged potential has an upper bound of -3 kV, while there are some oscillations due to the pulsed beam that cause a lower potential as well.

This pulsed control strategy has the benefits of the on-off pulsed beam described earlier, but does not improve the signal for both estimation methods due to the lack of energy pulsing. For energy pulsing control, the control law

$$I_{EB,0,k} = I_{EB,0,k-1} + K_c(\hat{\phi}_T - \phi_{T,des}) \tag{9}$$

is used to update the nominal beam current $I_{EB,0}$, with feedback gain K_c. The simulation results for closed-loop energy pulsing are shown in Fig. 8 for a desired potential of -3 kV and a feedback gain of $K_d = \cdot 10^{-5}$. The beam energy switches between 20 and 6 keV, and the pulse duty cycle and frequency are 0.5 and 5 Hz, respectively. In the simulation, the beam current settles just below 4 µA, resulting in the desired target potential. During the high energy phases, the target charges negatively and the high landing energy is favorable for the x-ray method. For the other half of one pulse cycle (due to the duty cycle of 0.5), the low beam energy results in a lower landing energy that causes the target to charge positively again. With this control, the beam energy levels for both the high and low phase could be adjusted to maintain favorable landing energies for each method.

IV. CONCLUSIONS

Two methods have been recently investigated that allow for the remote estimation of the electric potential of a nearby spacecraft by emitting an electron beam from a servicer and aiming the beam at the target. This excites x-rays and secondary electrons from the target that can be used for the estimation. However, the two methods benefit from dissimilar beam parameters. Pulsing the beam allows to quickly switch between beam settings that benefit one method at a time. This work showcases multiple ways of pulsing the beam to allow for better signals while sensing as well as charge control. Using on-off pulsing reduces the effective beam current delivered

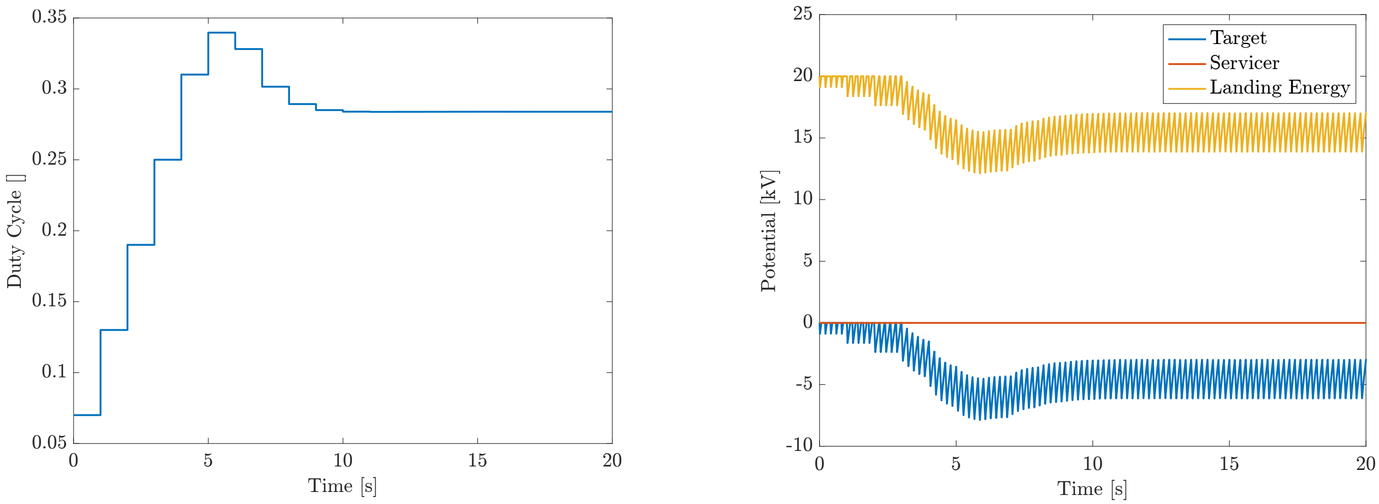

(a) Duty Cycle (b) Potentials

Fig. 7: Closed Loop On-Off Pulsing

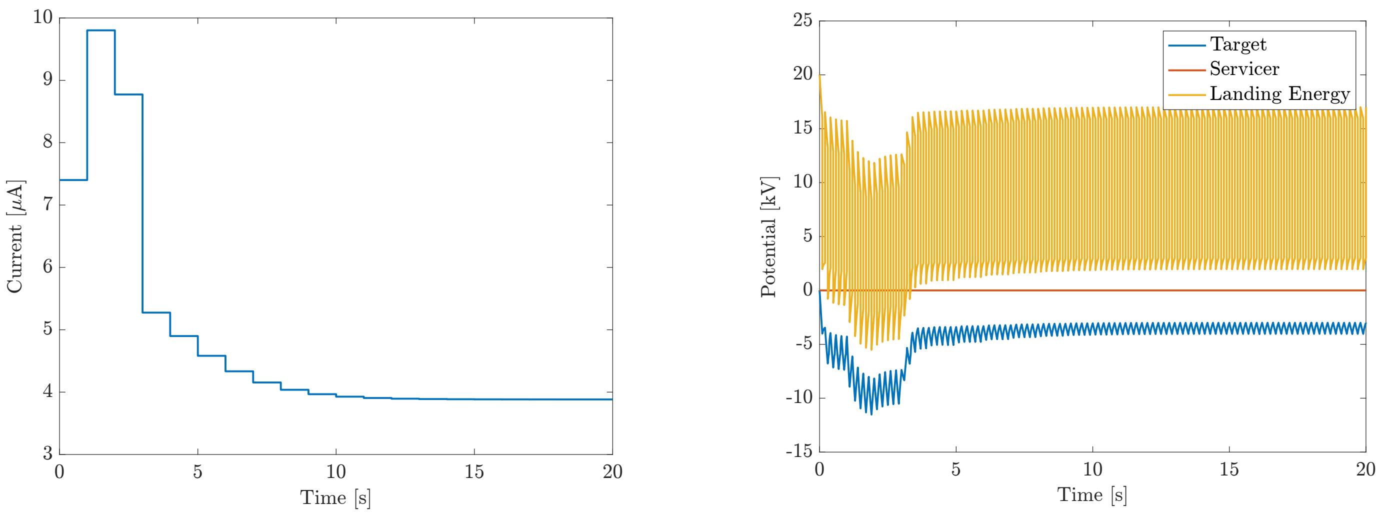

(a) Nominal Beam Current (b) Potentials

Fig. 8: Closed Loop Energy Pulsing

to the target, such that the target potential is perturbed less while sensing. Energy pulsing allows to switch between a low landing energy (beneficial for the secondary electron method) and high energy (beneficial for the x-ray method).

ACKNOWLEDGMENTS

This work was supported by U.S. Air Force Office of Scientific Research under grant FA9550-23-1-0570. Julian Hammerl gratefully acknowledges funding from the NASA FINESST fellowship (award number 80NSSC22K1849).

REFERENCES

[1] H. Schaub and Z. Sternovsky, “Active space debris charging for contactless electrostatic disposal maneuvers,” *Advances in Space Research*, vol. 53, no. 1, pp. 110–118, Jan. 2014.

[2] E. A. Hogan and H. Schaub, “Impacts of hot space plasma and ion beam emission on electrostatic tractor performance,” *IEEE Transactions on Plasma Science*, vol. 43, no. 9, pp. 3115–3129, 2015.

[3] ——, “Impacts of tug and debris sizes on electrostatic tractor charging performance,” *Advances in Space Research*, vol. 55, no. 2, pp. 630–638, 2015.

[4] J. A. Hughes and H. Schaub, “Electrostatic tractor analysis using a measured flux model,” *Journal of Spacecraft and Rockets*, vol. 57, no. 2, pp. 207–216, 2020.

[5] J. Hammerl and H. Schaub, “Coupled Spacecraft Charging Due to Continuous Electron Beam Emission and Impact,” *Journal of Spacecraft and Rockets*, 2024, accepted.

[6] K. Wilson and H. Schaub, “Impact of Electrostatic Perturbations on Proximity Operations in High Earth Orbits,” *Journal of Spacecraft and Rockets*, vol. 58, no. 5, pp. 1293–1302, 2021.

[7] ——, “Constrained guidance for spacecraft proximity operations under electrostatic perturbations,” in *IEEE Aerospace Engineering Conference*, Big Sky, MT, Mar. 2021, pp. 1–11.

[8] ——, “X-Ray Spectroscopy for Electrostatic Potential and Material Determination of Space Objects,” *IEEE Transactions on Plasma Science*, vol. 47, no. 8, pp. 3858–3866, Aug. 2019.

[9] M. Bengtson, J. Hughes, and H. Schaub, “Prospects and Challenges for Touchless Sensing of Spacecraft Electrostatic Potential Using Electrons,” *IEEE Transactions on Plasma Science*, vol. 47, no. 8, pp. 3673–3681, Aug. 2019.

[10] K. T. Wilson, M. T. Bengtson, and H. Schaub, “X-ray Spectroscopic Determination of Electrostatic Potential and Material Composition for Spacecraft: Experimental Results,” *Space Weather*, vol. 18, no. 4, pp. 1–10, Apr. 2020.

[11] J. Hammerl and H. Schaub, “Effects of Electric Potential Uncertainty on Electrostatic Tractor Relative Motion Control Equilibria,” *Journal of Spacecraft and Rockets*, vol. 59, no. 2, pp. 552–562, Mar. 2022.

[12] M. T. Bengtson, K. T. Wilson, and H. Schaub, “Experimental Results of Electron Method for Remote Spacecraft Charge Sensing,” *Space Weather*, vol. 18, no. 3, pp. 1–12, Mar. 2020.

[13] Á. Romero-Calvo, J. Hammerl, and H. Schaub, “Touchless Potential Sensing of Differentially Charged Spacecraft Using Secondary Electrons,” *Journal of Spacecraft and Rockets*, pp. 1–11, May 2022, in press.

[14] S. T. Lai, *Fundamentals of Spacecraft Charging*. Princeton University Press, Oct. 2011.

[15] Á. Romero-Calvo, G. Cano-Gómez, and H. Schaub, “Simulation and Uncertainty Quantification of Electron Beams in Active Spacecraft Charging Scenarios,” *Journal of Spacecraft and Rockets*, vol. 59, no. 3, pp. 739–750, May 2022.

[16] M. H. Denton, M. F. Thomsen, H. Korth, S. Lynch, J. C. Zhang, and M. W. Liemohn, “Bulk plasma properties at geosynchronous orbit,” *Journal of Geophysical Research: Space Physics*, vol. 110, no. A7, 2005.

[17] H. Schaub and D. F. Moorer, “Geosynchronous Large Debris Reorbiter: Challenges and Prospects,” *The Journal of the Astronautical Sciences*, vol. 59, no. 1-2, pp. 161–176, Jun. 2012.

[18] J. Hughes and H. Schaub, “Prospects of using a pulsed electrostatic tractor with nominal geosynchronous conditions,” *IEEE Transactions on Plasma Science*, vol. 45, no. 8, pp. 1887–1897, 2017.